

Clathrates of Group 14 with Alkali Metals: An Exploration

Svilen Bobev and Slavi C. Sevov

Department of Chemistry and Biochemistry, University of Notre Dame, Notre Dame, Indiana 46556-5670

E-mail: ssevov@nd.edu.

Received February 25, 2000; in revised form April 17, 2000; accepted April 20, 2000; published online July 11, 2000

The quantitative synthesis of four silicon and germanium compounds with the clathrate-II structure, $\text{Cs}_8\text{Na}_{16}\text{Si}_{136}$ (1), $\text{Cs}_8\text{Na}_{16}\text{Ge}_{136}$ (2), $\text{Rb}_8\text{Na}_{16}\text{Si}_{136}$ (3), and $\text{Rb}_8\text{Na}_{16}\text{Ge}_{136}$ (4), and their characterizations are reported. The corresponding Si–Si and Ge–Ge distances are determined with high accuracy from extensive single-crystal X-ray diffraction work. The compounds (cubic, space group $Fd\bar{3}m$, $a = 14.7560(4)$, $15.4805(6)$, $14.7400(4)$, and $15.4858(6)$ Å for 1, 2, 3, and 4, respectively) are stoichiometric, metallic, and remarkably stable. No evidence was found for vacancies in the silicon and germanium networks or partial occupancies of the alkali metal sites. The stoichiometry of these completely filled clathrates is consistent with the measured temperature-independent Pauli paramagnetism ($\chi = 7.2 \times 10^{-4}$, 6.5×10^{-4} , 6.9×10^{-5} , and 1.4×10^{-4} emu/mol for 1, 2, 3, and 4, respectively) and metallic resistivity ($\rho_{293} \approx 10^{-5}$ Ω-cm). © 2000 Academic Press

INTRODUCTION

The electronic revolution has brought great changes in every aspect of today's life. Undoubtedly, these changes were possible because the Si- and Ge-based electronic devices allowed miniaturization, functional integration, and low cost. However, the relatively small and indirect band gaps of the bulk Si and Ge make them unsuitable for many other potential applications. The dipole forbidden optical transition across the indirect energy gap hinders the light-emitting efficiency, limits large-scale optoelectronic integration, and prevents the realization of novel concepts. Considerable scientific attention has been focused on altering the electronic structure of these elements by introducing heteroatoms into the crystal structure, i.e., by doping them with appropriate elements to overcome the low radiative recombination probability (1). Extensive efforts for band structure engineering have focused on changing the bonding geometry, i.e., breaking the symmetry or the crystal periodicity (2). Recent developments in this area have led to fabrication of structures that are small enough to exploit quantum confinement effects and to show an increased radiative rate by emitting light at room temperature (3).

Ever since, semiconducting nanocrystals and porous materials have been extensively studied. It has been shown by theoretical calculations (4) and confirmed by experimental work (5) that making openings in the semiconducting structures widens the band gap and causes both valence and conduction bands to have extrema at the zone center. This brought to light the idea of making phases of group 14 elements with open framework structures, which are possible candidates for such optoelectronic applications.

It is not a simple task, however, to realize this idea in the case of silicon and germanium. They both crystallize in cubic face-centered diamond-type lattices and form two of the most stable and rigid covalent crystals known. Possible graphite modifications of Si and Ge are unstable and have never been experimentally prepared. Other structures can be achieved under high pressure, where transition from a four- to six-coordinated state occurs, and the semiconducting diamond-type lattice converts to a metallic β -Sn-type phase (6). To the best of our knowledge, expanded structures containing solely Si or Ge do not exist. The only open framework structures of Si and Ge are the so-called clathrates—inclusion compounds with open three-dimensional frameworks, made of tetrahedrally coordinated silicon or germanium atoms and voids that are occupied by alkali and alkaline-earth metals.

BACKGROUND

The story of the clathrates begins as early as 1811 when the first scientific report on a chlorine–ice compound with unidentified nominal composition that had earlier been thought to be crystalline chlorine appeared in the literature (7). Twelve years later *M. Faraday* revised the data and determined the stoichiometry to be $\text{Cl}_2(\text{H}_2\text{O})_{10}$ (8). It was another 148 years before the structure and the correct formula ($\text{Cl}_2(\text{H}_2\text{O})_{5.75}$) were determined (9) and the compound was described as a three-dimensional network of fused large polyhedra incorporating channels and cages occupied by the “guest impurities.” Meanwhile, a large number of similar compounds were synthesized (e.g., $\text{G}_8(\text{H}_2\text{O})_{46}$, where

TABLE 1

Up-to-Date List of Silicon, Germanium, and Tin Clathrate Compounds with Alkali (*A*) or Alkaline Earth (*AE*) Metals and Group 13 (*Tr*) or Group 12 (*E*) Elements (See Text)

<i>A-Tl</i>	Na ₈ Si ₄₆ (10), K ₈ Si ₄₆ (11), K ₈ Ge ₄₆ (11), K ₈ Sn ₄₆ (11), Rb ₈ Sn _{44.6(1)} (21), K _{1.6(2)} Cs _{6.4(2)} Sn _{44.0(1)} (21), Cs ₈ Sn ₄₆ (43) Na _x Si ₁₃₆ [3 < <i>x</i> < 11] (10), Na _x Ge ₁₃₆ (22), Na _x Si ₁₃₆ [1 < <i>x</i> < 23] (16,23) Cs ₈ Na ₁₆ Si ₁₃₆ (27), Cs ₈ Na ₁₆ Ge ₁₃₆ (27), Rb ₈ Na ₁₆ Si ₁₃₆ , ^a Rb ₈ Na ₁₆ Ge ₁₃₆ ^a
<i>AE-Tl</i>	(hp)Ba ₈ Si ₄₆ (29), Na _x Ba _y Si ₄₆ (28)
<i>A-Tr-Si</i>	K ₈ Al ₂₃ Si ₂₃ (48), Na ₈ Ga ₂₃ Si ₂₃ (48), K ₈ In ₁₈ Si ₂₈ (48), K ₈ Ga ₁₄ Si ₃₂ (48), K ₈ Ga ₈ Si ₃₈ (51), Rb ₈ Ga ₈ Si ₃₈ (49)
<i>A-Tr-Ge</i>	K ₈ Ga ₂₃ Ge ₂₃ (48), Na ₈ Ga ₁₆ Ge ₃₀ (48), K ₈ In ₁₆ Ge ₃₀ (48), K ₈ Al ₈ Ge ₃₈ (45), Rb ₈ Al ₈ Ge ₃₈ (58), Rb ₈ In ₈ Ge ₃₈ (46), Rb ₈ Ga ₈ Ge ₃₈ (49), Cs ₈ Ga ₈ Ge ₃₈ (59), Cs ₈ In ₈ Ge ₃₈ (61), K ₈ In ₈ Ge ₃₈ (46)
<i>A-Tr-Sn</i>	K ₈ Ga ₂₃ Sn ₂₃ (48), K ₈ In ₂₃ Sn ₂₃ (48), K ₈ Al ₂₃ Sn ₂₃ (48), K ₈ Ga ₈ Sn ₃₈ (51), K ₈ Al ₈ Sn ₃₈ (45), Rb ₈ Al ₈ Sn ₃₈ (58), Rb ₈ Ga ₈ Sn ₃₈ (49), Cs ₈ Ga ₈ Sn ₃₈ (59)
<i>A-E-Sn</i>	Cs ₈ Zn ₄ Sn ₄₂ (42)
<i>AE-Tr-Si</i>	Ba ₈ Ga ₁₆ Si ₃₀ (52), Ba ₈ Al ₁₆ Si ₃₀ (52), Sr ₈ Al ₁₆ Si ₃₀ (52), Sr ₈ Ga ₁₆ Si ₃₀ (52)
<i>AE-Tr-Ge</i>	Ba ₈ Ga ₁₆ Ge ₃₀ (52), Ba ₈ Al ₁₆ Ge ₃₀ (52), Sr ₈ Ga ₁₆ Ge ₃₀ (52), Ba ₈ In ₁₆ Ge ₃₀ (53)
<i>AE-E-Ge</i>	Ba ₈ Cd ₈ Ge ₃₈ (53), Ba ₈ Zn ₈ Ge ₃₈ (53)
<i>AE-TM-Si</i>	Ba ₈ TM _x Si _{46-x} [TM = Au, Ag, Cu] (57)
<i>AE-Tr-Sn</i>	β-Ba ₈ Ga ₁₆ Sn ₃₀ (50), Ba ₈ Ga ₃₂ Sn ₁₀₄ (26)
Other	X ₈ R ₈ Ge ₃₈ [X = Cl, Br, I; R = P, As, Sb] (54), I ₈ {I _x Ge _{46-x} } [x = 8/3] (56), I ₈ P _{19.3(2)} Sn ₂₄ (55), I ₈ As _{19.3(2)} Sn ₂₄ (55), Ba ₈ Cu ₁₆ P ₃₀ (60)

Note. *Italics* represent the clathrate-II phases. References in parentheses.

^aThis work.

G = Ar, Kr, Xe, H₂S, Cl₂, CH₄, and G₂₄(H₂O)₁₃₆ or G₁₆G₈(H₂O)₁₃₆ where *G* = H₂S, CO₂, CHCl₃, *n*-propane, nitromethane, cyclopentane, etc.) and were called gas and liquid hydrates (double hydrates) or often referred to as type I and type II clathrates, respectively. Almost a decade later, in 1965, the first clathrate compounds of Si with sodium were synthesized by “controlled thermal decomposition of the Zintl phase NaSi” and were structurally characterized (10). These compounds were Na₈Si₄₆ and Na_xSi₁₃₆, with the latter reported to be a nonstoichiometric phase with metal content varying between 3 and 11. The discovery of the silicon clathrates also stimulated more interest in compounds of C, Ge, Sn, and Pb with alkali metals. Efforts in this direction led to the discovery (1969) of the first germanium and tin clathrates of type I, K₈Ge₄₆ and K₈Sn₄₆, synthesized by direct fusion from pure elements (11). Since then, much experimental and theoretical work has been devoted to the clathrates of group 14 with alkali/alkaline earth metals. By 1991 5 binary and 17 ternary phases with clathrate-I structure and only 3 nonstoichiometric clathrate-II phases were reported (12). Theoretical calculations done in the late 1980s revealed that hypothetical carbon modifications with clathrate structures would have only about 0.07–0.09 eV less cohesive energy per atom than the diamond phase (13). Later, when *ab initio* DFT planewave pseudopotential methods were used, similar results were obtained for Si and Ge; i.e., Si and Ge clathrates are slightly less stable by about 0.07 and 0.05 eV per atom, respectively, relative to bulk pure elements (14). Thus, clathrates made of group 14 elements started to attract greater attention, and in the past 9 years the number of compositions with clathrate-type structures has increased by a factor of 2. There are now more than 50 phases with such struc-

tures reported, the vast majority of them being clathrate-I (Table 1). So far, there are no clathrates of carbon or lead known. For carbon, the reason is most likely its tendency for strong π-bonding and the possibility of forming polyhedra of even larger sizes such as the fullerene-like C₆₀ and the alkali-metal-doped A₃C₆₀ (15). For lead, perhaps the more pronounced metallic properties prevent the formation of localized covalent bonds as required for the clathrates.

The stoichiometries of the two types of clathrates do not differ much. When normalized, their ideal (completely filled) chemical formulas are AX_{5.75} and AX_{5.67}, for clathrates-I and -II, respectively. Structurally, however, they are noticeably different.

The prototypes of the clathrate-I structure are the gas hydrates with stoichiometry G₈(H₂O)₄₆, where *G* = Ar, Kr, Xe, H₂S, Cl₂, CH₄, etc. Clathrate-I phases crystallize in primitive cubic lattices (space group *Pm* $\bar{3}$ *n*, No. 223). The 46 clathrand atoms (oxygens from the water in this case) are all tetrahedrally coordinated and their arrangement in the unit cell is such that one can define two polyhedra of different sizes: one is a 20-atom pentagonal dodecahedron [5¹²], and the other is a 24-atom tetrakaidecahedron [5¹²6²] (the symbol [5¹²6²] denotes a polyhedron with 12 pentagonal and 2 hexagonal faces). The guest atoms or molecules can be encapsulated into these cages if their sizes are comparable to the size of the available empty space. Another feature of this structure is that the tetrakaidecahedra create a system of three mutually perpendicular “channels” by sharing common hexagonal faces. Three pairs of channels enclose the smaller dodecahedra and separate them from each other, as shown in Fig. 1. It is important to note that there are eight cages per formula unit, two smaller and six larger, and therefore the clathrate-I formula can be written as

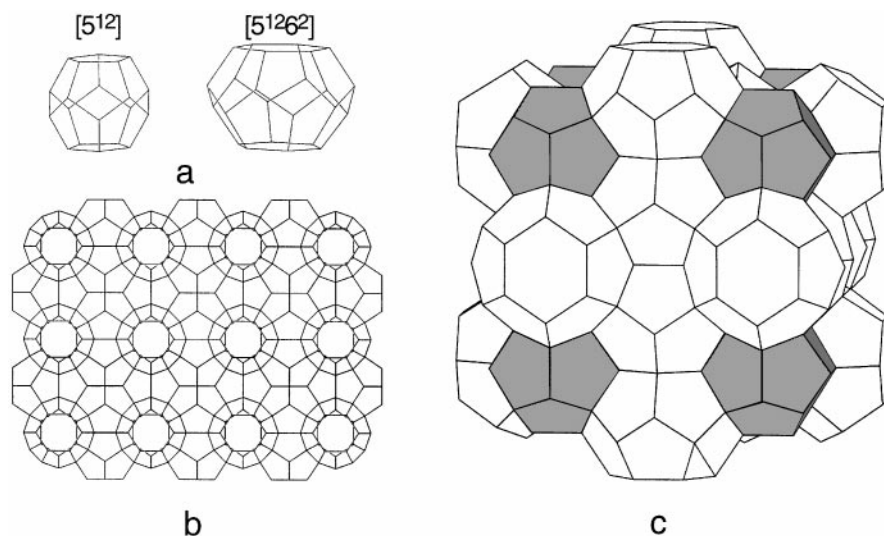


FIG. 1. (a) Building units of the clathrate-I structure, the 20-atom pentagonal dodecahedron $[5^{12}]$ with 12 pentagonal faces and the tetrakaidecahedra $[5^{12}6^2]$ with 12 pentagonal and 2 hexagonal faces; (b) clathrate-I layer; (c) polyhedral representation of the clathrate-I unit cell. The shaded polyhedra are the pentagonal dodecahedra, enclosed between the three mutually perpendicular channels of tetrakaidecahedra that share their hexagonal faces.

$G'_2 G''_6 X_{46}$, where X denotes the clathrand element (group 14 element or water molecule), and G' and G'' stand for the atoms/molecules occupying the $[5^{12}]$ and $[5^{12}6^2]$ polyhedra, respectively.

Clathrate-II crystallizes in the face-centered $Fd\bar{3}m$ cubic space group (No. 227). The parent compounds of this type are the liquid and double hydrates $G_{24}(\text{H}_2\text{O})_{136}$ and $G_{16}G_8(\text{H}_2\text{O})_{136}$, respectively, where $G = \text{H}_2\text{S}$, CO_2 , n -propane, nitromethane, cyclopentane, tetrachloromethane, etc.

Clearly, the molecules in this case are larger than the “guest species” in the clathrate-I structures. The framework-building atoms are again four-bonded in a nearly ideal tetrahedral environment and also form two different polyhedra. The key difference is that here, in addition to the pentagonal dodecahedron $[5^{12}]$, the second-type polyhedra are built of 28 atoms, hexakaidecahedra $[5^{12}6^4]$, that have 12 pentagonal and 4 hexagonal faces (Fig. 2). They are linked to each other by their hexagonal faces, forming a diamond-like

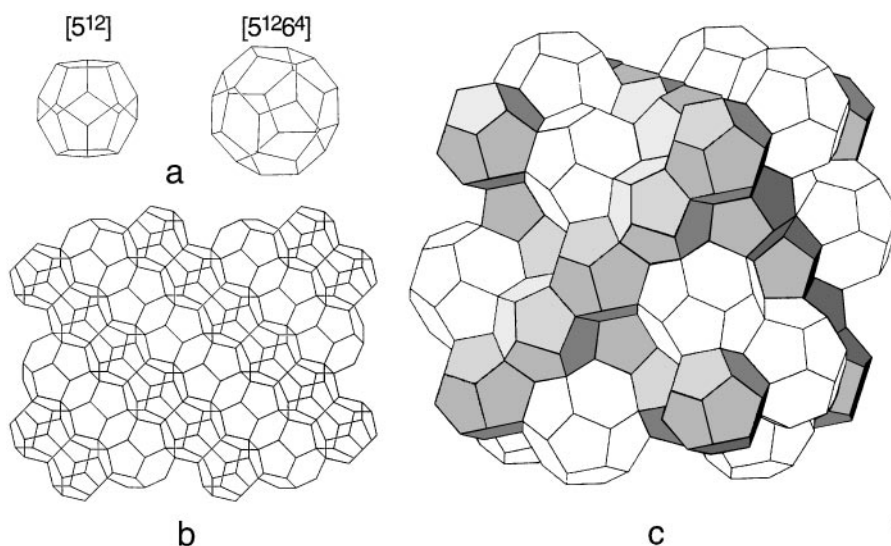


FIG. 2. (a) Building units of the clathrate-II structure, the 20-atom pentagonal dodecahedron $[5^{12}]$ with 12 pentagonal faces and the hexakaidecahedra $[5^{12}6^4]$ with 12 pentagonal and 4 hexagonal faces; (b) clathrate-II layer; (c) polyhedral representation of the clathrate-II unit cell. The shaded polyhedra are the pentagonal dodecahedra that are linked together. The hexakaidecahedra share their 4 hexagonal faces forming a diamond-like structure.

structure. The smaller pentagonal dodecahedra are not isolated as in the clathrate-I structure but are rather linked through common faces to form layers. The latter are stacked in an ABC sequence typical of cubic close packing, as shown in Fig. 2. The ratio of smaller to larger cavities in clathrate-II is 16:8 and therefore the formula can be written as $G'_{16}G''_8X_{136}$.

An analogy can also be drawn between the zeolites and the clathrates—the latter often being referred to as “zeolites without oxygen” or “oxygen-free zeolites” (14). Because of the many ways of linking $\text{SiO}_{4/2}$ tetrahedra in the zeolites via the rather flexible Si–O–Si angle, there are a great variety of zeolite structures, both naturally occurring and experimentally synthesized. Formal removal of the oxygen, i.e., replacement of the X–O–X bonding (X = Al, Si, Ge) with direct X–X bonds while preserving the tetrahedral coordination, and appropriate “rescaling” of the unit cell would result in the formation of isomorphous open frameworks. The bond energy of Si–Si or Ge–Ge is such that stretching the bonds and bending the angles are no longer favorable, and as a result, there are only two types of silicon or germanium clathrates, clathrate-I and clathrate-II, known thus far. Their structures are analogous with the structures of the melanophlogite and zeolite ZSM-39 (MTN or Dodecasil 3C), respectively. Another very important difference between the zeolites and the clathrates is that there are zeolite structures that are stable upon removal of the atoms or molecules occupying the channels and cages, whereas the clathrate structures collapse upon removal of the alkali metals.

According to Table 1, so far there are seven binary or pseudo-binary compounds between alkali metals and group 14 elements with the clathrate-I structure: $\text{Na}_8\text{Si}_{46}$, K_8Si_{46} , K_8Ge_{46} , K_8Sn_{46} , $\text{Cs}_8\text{Sn}_{46}$, $\text{Rb}_8\text{Sn}_{44.6(1)}$, and $\text{K}_{1.6(2)}\text{Cs}_{6.4(2)}\text{Sn}_{44.0(1)}$. The phase $\text{Na}_8\text{Si}_{46}$ was initially recognized from a X-ray powder diffraction pattern (10). Based on structure refinement and bulk elemental analysis (Na:Si \approx 1:6), the stoichiometry was determined to be 8:46 (1:5.75), in agreement with the ideal stoichiometric ratio and the measured metallic-like electric resistivity with room temperature values on the order of 10^{-2} – 10^{-3} Ω -cm. Recently, the ideal stoichiometry for $\text{Na}_8\text{Si}_{46}$ was confirmed by *Rietveld* analysis and ^{29}Si NMR work (16). The first single-crystal refinements of the clathrate-I structure were done on data collected with a Weissenberg camera for potassium compounds with Si, Ge, and Sn and were also refined as 8:46 (11). The latter led to a conflict with the reported semiconducting properties of K_8Ge_{46} ($\rho_{293} \approx 10^{-1}$ Ω -cm), a compound that had been thought to be isoelectronic with $\text{Na}_8\text{Si}_{46}$. The accuracy of the stoichiometry and the structure determination have been questioned ever since. The formal electronic structure can be derived from the Zintl–Klemm–Busmann concept; namely, each alkali metal atom is merely an electron donor and

transfers its valence electron to the Tt (Tt = Tetrel, i.e., group 14 element) network to become a cation. Each Tt, on the other hand, is bonded to four other Tt atoms and is therefore neutral. Thus, the clathrate-I phase with ideal stoichiometry 8:46 should be a conductor because of the eight extra electrons per formula from the eight alkali metals. Nevertheless, as mentioned above, property measurements suggest that the clathrate-I phases can be diamagnetic and semiconducting instead of metallic. For a long time A_8Tt_{46} compounds were considered examples of the metal-to-insulator *Mott* transition (17). However, the explanation for these properties is the formation of defects in the four-bonded Tt_{46} network (18–20). A missing Tt atom will leave the four neighboring atoms with incomplete valence shells; i.e., four extra electrons will be needed to complete their octet configurations with lone pairs. Two vacancies per formula will translate to $2 \times (-4) = -8$ negative charges, and this equals the number of donated electrons by the eight alkali metals. Thus, the compound becomes electronically balanced and provides a nice agreement between experimental data and theory. Only more recent single-crystal work on clathrate-I compounds in the binary Rb–Sn and pseudo-binary (K,Cs)–Sn systems has shown that indeed one of the framework sites is partially occupied, and the stoichiometry $\text{A}_8\text{Sn}_{44}\square_2$ represents the correct and electronically balanced formula for a Zintl compound with two Sn vacancies (\square) per formula (21). Another way to balance the “extra” charges from the alkali metals is to substitute Tt atoms from the network with an electron-poorer element, from group 13 or 12, for example. This idea has been widely used in the past 10–15 years to make new ternary phases with the clathrate-I structure. The ideal stoichiometries will be $\text{A}_8\text{Tr}_8\text{Tt}_{38}$ and $\text{A}_8\text{E}_4\text{Tt}_{42}$ or $[\text{AE}]_8\text{Tr}_{16}\text{Tt}_{30}$ and $[\text{AE}]_8\text{E}_8\text{Tt}_{38}$, where A = alkali, AE = alkaline earth, Tr (Triel) = group 13, and E = group 12 elements. The existence of many of these compositions and their compliance with the Zintl concept have been proven (Table 1). Nonetheless, there are many controversial results such as $\text{A}_8\text{Tr}_{23}\text{Tt}_{23}$, $\text{A}_8\text{Tr}_{16}\text{Tt}_{30}$, and $\text{A}_{8-x}[\text{AE}]_x\text{Tt}_{46}$ that neither fit into the above-mentioned scheme nor fulfill the Zintl requirements.

Even more complicated and difficult for interpretation are the compounds with the clathrate-II type structure. Until recently, only the nonstoichiometric $\text{Na}_x\text{Si}_{136}$ and $\text{Na}_x\text{Ge}_{136}$ phases were known in the binary A–Tt systems (10,22). Initially, for $\text{Na}_x\text{Si}_{136}$, the sodium content x was reported to vary between 3 and 11, but later the range of the domain compositions was broadened to lower ($x = 1$) and higher ($x = 23$) concentrations (16,23). There have been speculations that this nonstoichiometric phase also undergoes insulator-to-metal *Mott* transition at $x \approx 10$ (22–24). Later, it was shown by ^{23}Na NMR that the transition can occur, even at $x < 9$ (25). The same authors also suggested that the large ^{23}Na *Knight* shifts and broad NMR peaks for

$\text{Na}_x\text{Si}_{136}$ at $x < 9$ can be attributed to localized alkali metal electrons. Also, the $\text{Na}_x\text{Si}_{136}$ structure was refined from X-ray powder diffraction with the aid of the *Rietveld* method to determine the distribution of the sodium atoms within the two available alkali metal sites, i.e., the centers of the pentagonal dodecahedra and the hexakaidecahedra (16,23). It was concluded that, for $x \leq 8$, the Na atoms occupy preferably the larger $[5^{12}6^4]$ cage. Unlike clathrate-I, substitution of the *Tt* atoms with triel and other elements has not led to as many ternary compounds. Only the structure of $\text{Ba}_{16}\text{Ga}_{32}\text{Sn}_{104}$ has been reported but with extensive disorder of Sn and Ga on all crystallographic sites (26). The structure refinement has given the composition $\text{Ba}_{16}\text{Ga}_x\text{Sn}_{136-x}$, where $x = 32 \pm 1.4$, and no indication for potassium content, although the reaction mixture includes K, Ba, Ga, and Sn. The refinement indicates that the Ba cations occupy only the smaller cages while the larger ones remain empty. No elemental analysis, resistivity, or magnetic measurements have been done to prove the authors' conclusion that the compound is electronically balanced and belongs to the Zintl phases. Until very recently, there was no unequivocal structure determination for compounds with the clathrate-II structure. The first well-refined structures and reproducible direct syntheses were reported for the stoichiometric and completely filled silicon and germanium clathrate-II compounds $\text{Cs}_8\text{Na}_{16}\text{Si}_{136}$ and $\text{Cs}_8\text{Na}_{16}\text{Ge}_{136}$ (27).

The interest in clathrates jumped abruptly even higher after the unexpected discovery of superconductivity in the clathrate-I compounds $\text{Ba}_y\text{Na}_x\text{Si}_{46}$ and $\text{Ba}_8\text{Si}_{46}$ (28,29). It was unprecedented because no other examples of superconductivity were known for phases with covalent sp^3 bonding. More recent research showed that the silicon clathrates have low compressibility and therefore are considered potential superhard materials (30). In addition, it was hypothesized that variable physical properties such as the *Seebeck* coefficient or thermopower (S) and the electrical (σ) and thermal (λ) conductivities may be tuned by altering the guest atoms in the cages. This brought new motivation for clathrate studies as potential thermoelectric materials. The stability of the clathrates, the fact that they conduct electricity relatively well, and the possibility of "rattling" guest cations in the cavities bring the clathrates closer to the ultimate thermoelectric PGEC ("phonon-glass and an electron crystal") material, a concept introduced by *Slack* in 1979 (31). To increase the figure of merit ZT , an empirical coefficient that measures the thermoelectric performance (T = temperature and $Z = \sigma S^2/\lambda$), one needs material with high thermopower and low thermal conductivity. The latter has two components—thermal electronic conductivity that is proportional to the electrical conductivity (no more than 5% of the total λ) and lattice thermal conductivity. Clearly, since the electrical conductivity and the electronic component of the thermal conductivity cannot be varied indepen-

dently, a higher figure of merit can be expected for material with low lattice thermal conductivity. Si and Ge clathrates are considered promising candidates for thermoelectric applications since their relatively large unit cells with "voids and rattlers inside them" are important prerequisites for scattering of the heat-carrying phonons and thereby for low phonon-contributed thermal lattice conductivity. All this interest has led to the search for reliable and reproducible ways for the synthesis of all clathrates in high yields and with defined stoichiometry. Here, we report the direct synthesis of four new members of the clathrate-II family, $\text{Cs}_8\text{Na}_{16}\text{Si}_{136}$ (**1**), $\text{Cs}_8\text{Na}_{16}\text{Ge}_{136}$ (**2**), $\text{Rb}_8\text{Na}_{16}\text{Si}_{136}$ (**3**), and $\text{Rb}_8\text{Na}_{16}\text{Ge}_{136}$ (**4**), their single-crystal structural characterization, and magnetic and transport properties.

EXPERIMENTAL

Synthesis. All manipulations were performed inside a nitrogen-filled glove box with the moisture level below 1 ppm (vol). The starting materials were Na (Alfa, ingot, 99.9% metal basis), Cs (Acros, 99.95%), Rb (Alfa, 99.8% metal basis), Si (Alfa, lump, 99.9999% metal basis), and Ge (Acros, powder, 99.999%). The sodium surface was cleaned with a scalpel immediately before use. The four compounds were synthesized from reactions loaded with the exact stoichiometric ratio 8:16:136 and intended to yield clathrate-II phases. The mixtures were loaded in niobium containers that were subsequently arc-welded in an Ar-filled chamber. The prepared "reaction vessels" were then sealed in fused silica jackets under vacuum at ca. 10^{-5} mm Hg (below discharge). The reactions were carried out at 650°C for 3 weeks. At higher temperatures Si and Ge readily react with Nb, forming the stable phases NbSi_2 and NbGe_2 , and this causes leaks of alkali metals into the silica container. At 650°C neither Si nor Ge melts, and therefore, more time was needed to ensure better diffusion of the alkali metals into the silicon and germanium for this inhomogeneous system (32). The products of both reactions were well-shaped crystals with triangular faces, typical of compounds with F-centered cubic lattices, and had a distinctive bluish metallic luster. The yields were quantitative and the crystals were easily washed with deionized water and ethyl alcohol and separated under a microscope from the traces of unreacted dust-like Si and Ge or eventually NbSi_2 and NbGe_2 .

X-ray diffraction studies. X-ray powder diffraction patterns were taken on an Enraf-Nonius Guinier camera with $\text{CuK}\alpha_1$ radiation. Powder patterns of the product, before and after it was washed with water or heated under dynamic vacuum, did not show any differences in the line intensities and positions. The patterns were also used to verify the unit cell parameters by a least-squares refinement of the

positions of the lines, calibrated by silicon (NIST) as an internal standard.

Single-crystal diffraction data were collected on an Enraf-Nonius CAD-4 diffractometer with graphite monochromated MoK α radiation at room temperature. A few crystals were selected from each compound, mounted on quartz fibers, and checked for singularity. For the best ones, $0.20 \times 0.20 \times 0.20$ mm for Cs₈Na₁₆Si₁₃₆ ($2\theta_{\max} = 90^\circ$), $0.20 \times 0.12 \times 0.10$ mm for Cs₈Na₁₆Ge₁₃₆ ($2\theta_{\max} = 100^\circ$), $0.16 \times 0.12 \times 0.08$ mm for Rb₈Na₁₆Si₁₃₆ ($2\theta_{\max} = 50^\circ$), and $0.08 \times 0.04 \times 0.04$ mm for Rb₈Na₁₆Ge₁₃₆ ($2\theta_{\max} = 50^\circ$), data were collected with ω - 2θ scans in one octant for **1**, **2**, and **3** and in a full sphere for **4**. The data for **1**, **2**, and **3** were corrected for absorption using the average of three ψ -scans in each, while the data for **4** were treated with DIFABS (Xabs) due to the lack of good ψ -scan reflections. The structures were solved and refined on F^2 with the aid of the SHELXTL-V 5.1 software package (33). As expected, the refinements confirmed the clathrate-II structure and stoichiometry ($Fd\bar{3}m$ space group (No. 227)) without any partially occupied network sites or disorder for the alkali metals sites. Our previous work on **1** and **2** revealed that the refinements on the data collected for crystals before and after being treated with water, alcohol, acids, and heat and being treated hydrothermally are virtually identical (27) (within the standard deviation of less than 2.2σ). The list of

important crystallographic parameters and details for the refinements of the four compounds are summarized in Table 2. The final positional and equivalent isotropic displacement parameters and important distances are listed in Tables 3 and 4, respectively.

Property measurements. Magnetic measurements were carried out on a Quantum Design MPMS SQUID magnetometer at a field of 3 T over a temperature range of 10–270 K. Tests for superconductivity were also performed at a field of 0.1 or 0.3 T in the temperature range 2–10 K. The samples (17 mg of **1**, 18 mg of **2**, 58 mg of **3**, and 72 mg of **4**) were prepared by selecting crystals under microscope and subsequently checking their quality by powder XRD.

Four-probe resistivity measurements (van der Pauw's method) were made on single crystals and pellets using a home made set up and Hewlett-Packard 3457A digital multimeter. Thin platinum wires (1 μ m in diameter) were "glued" inline to the surface of the measured material with a silver paste. The crystal or the pellet with the attached probes was then mounted on the top of a chip, which was then connected to the multimeter with the aid of four coaxial wires. Reliable and reproducible data can be acquired within the resistivity range from 100 M Ω to 100 $\mu\Omega$. The pellets for the measurements were prepared from

TABLE 2
Selected Crystallographic Parameters for Cs₈Na₁₆Si₁₃₆, Cs₈Na₁₆Ge₁₃₆, Rb₈Na₁₆Si₁₃₆, and Rb₈Na₁₆Ge₁₃₆

	Na ₂ CsSi ₁₇	Na ₂ CsGe ₁₇	Na ₂ RbSi ₁₇	Na ₂ RbGe ₁₇
Empirical formula	Na ₂ CsSi ₁₇	Na ₂ CsGe ₁₇	Na ₂ RbSi ₁₇	Na ₂ RbGe ₁₇
Formula weight	656.42	1412.92	608.98	1365.48
Wavelength (Å), MoK α			0.71073	
Crystal system			Cubic	
Space group, No.			$Fd\bar{3}m$, 227	
Unit cell dimensions (Å)	$a = 14.7560(4)$	$a = 15.4805(6)$	$a = 14.7400(4)$	$a = 15.4858(6)$
Volume (Å ³), Z	3212.9(2), 8	3709.8(2), 8	3202.5(2), 8	3713.6(2), 8
Density (calculated, g/cm ³)	2.714	5.059	2.526	4.885
Absorption coefficient (cm ⁻¹)	36.06	290.41	43.97	296.83
Absorption correction	ψ -scan	ψ -scan	ψ -scan	Xabs
θ range (deg)	2.39–44.90	2.28–49.95	2.39–24.86	2.28–24.99
Limiting indices	$0 \leq hkl \leq 29$	$0 \leq hkl \leq 33$	$0 \leq hkl \leq 17$	$-16 \leq hkl \leq 18$
Reflections collected	3322	4864	706	1370
Independent reflections	680	977	165	188
	$[R_{\text{int}} = 0.0256]$	$[R_{\text{int}} = 0.1178]$	$[R_{\text{int}} = 0.0570]$	$[R_{\text{int}} = 0.0770]$
Data/restraints/parameters	680/0/15	977/0/15	165/0/15	188/0/15
Goodness-of-fit on F^2	1.202	1.033	1.061	1.103
Final R^a indices [$I > 2\sigma_I$](%)	$R_1 = 2.01$ $wR_2 = 4.53$	$R_1 = 4.31$ $wR_2 = 8.30$	$R_1 = 1.69$ $wR_2 = 3.91$	$R_1 = 2.75$ $wR_2 = 5.49$
R indices [all data] (%)	$R_1 = 2.31$ $wR_2 = 4.61$	$R_1 = 9.24$ $wR_2 = 9.81$	$R_1 = 2.06$ $wR_2 = 4.08$	$R_1 = 3.09$ $wR_2 = 5.57$
Extinction coefficient	0.00015(3)	0.00016(2)	0.00005(4)	0.00002(2)
Largest diff. peak (e/Å ³)	0.773	1.857	0.251	0.784
hole	-0.517	-2.019	-0.176	-0.676
Weight coefficient A/B	0.0183/1.8215	0.0356/8.7128	0.0000/5.3098	0.0262/1.7491

^a $R_1 = [\sum \|F_o\| - |F_c|] / \sum F_o$; $wR_2 = \{[\sum w(F_o)^2 - (F_c)^2] / [\sum w(F_o)^2]\}^{1/2}$; $w = [\sigma^2(F_o)^2 + (AP)^2 + BP]^2$, where $P = [(F_o)^2 + 2(F_c)^2]/3$.

TABLE 3

Atomic Coordinates and Equivalent Isotropic Displacement Parameters (U_{eq})^a for $Cs_8Na_{16}Si_{136}$, $Cs_8Na_{16}Ge_{136}$, $Rb_8Na_{16}Si_{136}$, and $Rb_8Na_{16}Ge_{136}$

Atom	Site	x	y	z	U_{eq} [\AA^2]
$Cs_8Na_{16}Si_{136}$					
Si1	96g	0.06768(1)	x	0.37022(1)	0.00664(5)
Si2	32e	0.21728(2)	x	x	0.00666(6)
Si3	8a	1/8	1/8	1/8	0.0066(1)
Na	16c	0	0	0	0.0187(2)
Cs	8b	3/8	3/8	3/8	0.01990(6)
$Cs_8Na_{16}Ge_{136}$					
Ge1	96g	0.06783(2)	x	0.37038(3)	0.0110(1)
Ge2	32e	0.21772(3)	x	x	0.01038(1)
Ge3	8a	1/8	1/8	1/8	0.0099(2)
Na	16c	0	0	0	0.034(1)
Cs	8b	3/8	3/8	3/8	0.0344(3)
$Rb_8Na_{16}Si_{136}$					
Si1	96g	0.06756(3)	x	0.37058(4)	0.0094(3)
Si2	32e	0.21752(4)	x	x	0.0092(3)
Si3	8a	1/8	1/8	1/8	0.0087(5)
Na	16c	0	0	0	0.0210(6)
Rb	8b	3/8	3/8	3/8	0.0314(3)
$Rb_8Na_{16}Ge_{136}$					
Ge1	96g	0.06770(4)	x	0.37071(5)	0.0132(4)
Ge2	32e	0.21794(4)	x	x	0.0122(4)
Ge3	8a	1/8	1/8	1/8	0.0104(6)
Na	16c	0	0	0	0.021(2)
Rb	8b	3/8	3/8	3/8	0.054(1)

^a U_{eq} is defined as one-third of the trace of the orthogonalized U_{ij} tensor.

carefully picked single crystals, which were then ground and pressed under a pressure of 100 ton in a $\frac{1}{2}$ -in. die at room temperature and at 200°C. Only a cold-pressed pellet was measured at different temperatures in the range of 10–300 K. It revealed progressively diminishing resistivity with decreasing temperature, which indicates metallic-like behavior. Nevertheless, due to the grain boundaries, the measurements at room temperature of this pellet were 2 orders of magnitude higher than those of the hot-pressed pellet and the single crystal. For the latter, on the other hand, measurements could be done only at room temperature because the resistivity of the samples went out of the range of the digital multimeter when the temperature was lowered. Independent conductivity measurements were also performed on monodisperse (particle size within the range of 250–425 μm) selected single crystals of $Cs_8Na_{16}Ge_{136}$ using a standard, high-frequency, contact-free Q-technique.

TABLE 4

Important Distances (\AA) in $Cs_8Na_{16}Si_{136}$, $Cs_8Na_{16}Ge_{136}$, $Rb_8Na_{16}Si_{136}$, and $Rb_8Na_{16}Ge_{136}$

$Cs_8Na_{16}Si_{136}$			$Rb_8Na_{16}Si_{136}$		
Si1–	Si1	2.3809(2) \times 2	Si1–	Si1	2.3728(7) \times 2
	Si1	2.3924(5)		Si1	2.395(1)
	Si2	2.3717(2)		Si2	2.3716(7)
Si2–	Si1	2.3717(2) \times 3	Si2–	Si1	2.3716(7) \times 3
	Si3	2.3584(4)		Si3	2.362(1)
Si3–	Si2	2.3584(4) \times 4	Si3–	Si2	2.362(1) \times 4
Na–	Si1	3.3738(2) \times 12	Na–	Si1	3.3737(4) \times 12
	Si2	3.2781(2) \times 6		Si2	3.2770(4) \times 6
	Si3	3.1948(1) \times 2		Si3	3.1913(1) \times 2
	Na	5.2170(1)		Na	5.2114(7)
	Cs	6.1175(2)		Rb	6.1109(2)
Cs–	Si1	3.9452(2) \times 12	Rb–	Si1	3.9367(6) \times 12
	Si1	4.0214(3) \times 12		Si1	4.0147(7) \times 12
	Si2	4.0311(4) \times 4		Si2	4.0205(9) \times 4
	Cs	6.3859(2)		Rb	6.3826(2)
$Cs_8Na_{16}Ge_{136}$			$Rb_8Na_{16}Ge_{136}$		
Ge1–	Ge1	2.4980(4) \times 2	Ge1–	Ge1	2.4932(8) \times 2
	Ge1	2.5033(9)		Ge1	2.510(1)
	Ge2	2.4881(5)		Ge2	2.4911(9)
Ge2–	Ge1	2.4881(5) \times 3	Ge2–	Ge1	2.4911(9) \times 3
	Ge3	2.4860(7)		Ge3	2.493(1)
Ge3–	Ge2	2.4860(7) \times 4	Ge3–	Ge2	2.493(1) \times 4
Na–	Ge1	3.5395(3) \times 12	Na–	Ge1	3.5444(5) \times 12
	Ge2	3.4437(3) \times 6		Ge2	3.4472(5) \times 6
	Ge3	3.3516(1) \times 2		Ge3	3.3528(1) \times 2
	Na	5.4732(2)		Na	5.4751(2)
	Cs	6.4179(2)		Rb	6.4201(3)
Cs–	Ge1	4.1356(4) \times 12	Rb–	Ge1	4.1331(8) \times 12
	Ge1	4.2222(5) \times 12		Ge1	4.2192(7) \times 12
	Ge2	4.2173(7) \times 4		Ge2	4.211(1) \times 4
	Cs	6.7033(3)		Rb	6.7055(3)

The thermopower of a hot-pressed pellet of $Cs_8Na_{16}Si_{136}$ was measured by using a steady-state technique over the temperature range 70–300 K.

RESULTS AND DISCUSSION

The unit cell parameters of the two Si clathrates, $a = 14.7560(4)$ and $14.7400(4)$ \AA for $Cs_8Na_{16}Si_{136}$ and $Rb_8Na_{16}Si_{136}$, respectively, are slightly larger than those reported for the nonstoichiometric Na_xSi_{136} phase ($1 < x < 23$), $a = 14.6428(4)$ and $14.7030(5)$ \AA for the lowest and highest sodium content, respectively. The latter are consistent with the suggested increase of the unit cell parameters with increasing alkali metal concentration (23). Theoretically optimized values for imaginary empty clathrate-II structures range between 14.46 and 14.86 \AA , depending largely on the computational method, and cannot be used for comparison (34). For the Ge analogs, on the other hand, only a theoretical value of $a = 15.13$ \AA for the empty Ge_{136}

TABLE 5
Standard and Variable Site Occupation Factors (SOF) and Equivalent Isotropic Displacement Parameters (U_{eq})^a for $Cs_8Na_{16}Si_{136}$, $Cs_8Na_{16}Ge_{136}$, $Rb_8Na_{16}Si_{136}$, and $Rb_8Na_{16}Ge_{136}$

Atom	Wyckoff site	Standard occupancies		Variable occupancies ^b	
		SOF	U_{eq} [\AA^2]	SOF	U_{eq} [\AA^2]
$Cs_8Na_{16}Si_{136}$					
Si1	96g	0.50000	0.00664(5)	0.500(1)	0.00662(7)
Si2	32e	0.16667	0.00666(6)	0.1672(5)	0.00674(9)
Si3	8a	0.04167	0.0066(1)	0.0413(3)	0.0064(2)
Na	16c	0.08333	0.0187(2)	0.0816(5)	0.018(3)
Cs	8b	0.04167	0.01990(6)	0.04175(8)	0.01994(6)
$Cs_8Na_{16}Ge_{136}$					
Ge1	96g	0.50000	0.0110(1)	0.495(3)	0.0108(1)
Ge2	32e	0.16667	0.01038(1)	0.168(1)	0.0108(2)
Ge3	8a	0.04167	0.0099(2)	0.0423(4)	0.0105(3)
Na	16c	0.08333	0.034(1)	0.084(2)	0.035(2)
Cs	8b	0.04167	0.0344(3)	0.04213(8)	0.0349(4)
$Rb_8Na_{16}Si_{136}$					
Si1	96g	0.50000	0.0094(3)	0.502(3)	0.0095(3)
Si2	32e	0.16667	0.0092(3)	0.167(1)	0.0092(5)
Si3	8a	0.04167	0.0087(5)	0.0429(6)	0.0100(9)
Na	16c	0.08333	0.0210(6)	0.0821(8)	0.0200(9)
Rb	8b	0.04167	0.0314(3)	0.0417(2)	0.0314(4)
$Rb_8Na_{16}Ge_{136}$					
Ge1	96g	0.50000	0.0132(4)	0.484(7)	0.0133(4)
Ge2	32e	0.16667	0.0122(4)	0.163(3)	0.0124(5)
Ge3	8a	0.04167	0.0104(6)	0.0399(9)	0.0096(5)
Na	16c	0.08333	0.021(2)	0.091(3)	0.029(3)
Rb	8b	0.04167	0.054(1)	0.0422(2)	0.055(2)

^a U_{eq} is defined as one-third of the trace of the orthogonalized U_{ij} tensor.

^b The occupancies of each site were freed while the remaining were kept fixed.

structure is available (35). Practically no other data, except the briefly mentioned but not further discussed phase Na_xGe_{136} with $a = 15.4 \text{ \AA}$, are known for the germanium type II clathrates (22). The calculated lattice parameter for the empty germanium clathrate is somewhat smaller (2.3% error) than the experimental values of the completely filled compounds, $a = 15.4805(6)$ and $15.4858(6) \text{ \AA}$ for $Cs_8Na_{16}Ge_{136}$ and $Rb_8Na_{16}Ge_{136}$, respectively. At the same time, the energy difference between the structure with the experimental coordinates and the one with optimized coordinates is only 1.3 meV/atom (35).

The structure refinements for all four systems unambiguously show that there are no partially occupied positions, both at the network and at the alkali metal sites (Table 5). Varying the occupancies of any Si or Ge site while keeping the remaining ones fixed does not lead to deviations of more than 2.2σ . Larger deviations (up to 5σ) were observed for the two alkali metal sites for all four clathrates. At the same time, their equivalent isotropic displacement parameters (U_{eq}) tended to increase slightly (within less than 2.5σ) with

varying site occupation, which can be attributed to either static disorder or vibration of the atom about its equilibrium position. The refinements with fractional occupancies or disorder of the alkali metal sites did not improve the overall structural parameters, and therefore the final least-squares cycles were done with 100% occupancies of all crystallographic sites. Since the data sets for $Cs_8Na_{16}Si_{136}$ and $Cs_8Na_{16}Ge_{136}$ were collected up to $2\theta = 90^\circ$ and 100° , respectively, while those for $Rb_8Na_{16}Si_{136}$ and $Rb_8Na_{16}Ge_{136}$ were collected up to 50° , the accuracy of the Cs compounds is clearly better.

The refinements confirm that the completely filled clathrate-II structure is rigid and invariant with respect to the size of the cation. The Si–Si distances range from 2.3584(4) to 2.3924(5) \AA for **1** and from 2.362(1) to 2.395(1) \AA for **3**. The corresponding ranges for the Si angles are from $105.52(1)^\circ$ to $119.842(2)^\circ$ in **1** and from $105.44(3)^\circ$ to $119.836(5)^\circ$ in **3**, the largest angles occurring at the six-member rings of the hexakaidecahedra. For the Ge compounds, the Ge–Ge distances range from 2.4859(7) to

TABLE 6

Approximate van der Waals Radii of the Empty Space^a in the Small ([5¹²]-Polyhedra) and Large ([5¹²6²]- or [5¹²6⁴]-Polyhedra) Cages for Silicon, Germanium, and Tin Clathrate Compounds, Compared with the Ionic Radii^b of the Alkali Metals (Å)

	Clathrate-I				Clathrate-II			
	Small cage		Large cage		Small cage		Large cage	
Si	1.10	Na	1.35	Na, K	1.10	Na	1.85	Rb, Cs
Ge	1.25	Na, K	1.55	K, Rb	1.25	Na, K	2.00	Rb, Cs
Sn	1.65	Rb, Cs	1.85	Rb, Cs	1.65	Rb, Cs	> 2.2(est.)	

Ionic radii for the alkali metals for CN = 6:
Na = 1.02, K = 1.38, Rb = 1.49, Cs = 1.70

^a Calculated based on the shortest *A-Tt* distances by subtracting the corresponding van der Waals radii for the Si, Ge, and Sn, respectively.

^b The values are those of Shannon and Prewitt (62), calculated for oxides (based on the value 1.40 Å for six-coordinated O²⁻). A certain allowance should be made due to the different coordination numbers of the alkali metal cations in the clathrate cages.

2.5033(9) Å and from 2.4911(9) to 2.510(1) Å for **2** and **4**, respectively, and the Ge angles are in the ranges from 105.22(2)° to 119.816(3)° and from 105.18(4)° to 119.809(6)° for the two compounds, respectively. Both Si-Si and Ge-Ge distances are somewhat longer than those in the pure elements, 2.352 Å for Si and 2.445 Å for Ge. Clearly, the reason for this is not the size of the cations since: (i) there is practically no change in the distances moving from Cs to Rb and (ii) the voids are larger than the alkali metal cations (Table 6). The most likely reasons for the longer distances in the clathrates are (i) the 24 extra electrons per 136 network atoms and (ii) the distorted tetrahedral environment since the deviations from the ideal tetrahedral angle 109.47° are not negligible.

The extra electrons could be either delocalized over the four-bonded network or localized on the alkali metals. The latter are well separated in this structure, 5.2170(1), 6.1175(2), and 6.3859(2) Å for the closest Na-Na, Cs-Na, and Cs-Cs contacts, respectively, in **1**; 5.4732(2), 6.4179(2), and 6.7033(3) Å for the closest Na-Na, Cs-Na, and Cs-Cs contacts, respectively, in **2**; 5.2114(7), 6.1109(2), and 6.3826(2) Å for the closest Na-Na, Rb-Na, and Rb-Rb contacts, respectively, in **3**; and 5.4751(2), 6.4201(3), and 6.7055(3) Å for the closest Na-Na, Rb-Na, and Rb-Rb contacts, respectively, in **4**. Thus, no interaction between them should be expected (the metallic radii for Na, Rb, and Cs are 1.90, 2.48, and 2.67 Å, respectively) (36). Nevertheless, based on EPR and NMR experiments, some authors speculate that the “system is better described in terms of encapsulated neutral alkali metal atoms, rather than one, containing Na⁺ ions” (16,23–25,37), i.e., systems with no electron transfer over the Si or Ge network but rather with

isolated free alkali metal atoms. This conclusion seems to be applicable only to the nonstoichiometric phase Na_xSi₁₃₆ and only at low Na concentrations (*x* < 9), since at higher Na concentrations insulator-to-metal transition occurs. Theoretical calculations using the full-potential all electron linear augmented plane wave method (FLAPW) indicate that, indeed, the sodium electrons are fairly localized at low alkali metal content (e.g., Na₄Si₁₃₆) but are delocalized at higher alkali metal concentrations (e.g., full occupation of all sites Na₂₄Si₁₃₆), due to significant overlap between the Na and Si orbitals (38). Thus, the extra alkali metal electrons in our case can be considered delocalized and partially filling the silicon or germanium conduction bands, which, of course, are composed of predominantly Si-Si or Ge-Ge antibonding states. This is also in agreement with the fact that the observed distances are also longer than those theoretically calculated for the empty clathrate-II structures.

Due to the extra 24 electrons per formula, all four compounds should be metallic conductors. Our preliminary four-probe conductivity measurements (cold-pressed pellets) for Cs₈Na₁₆Si₁₃₆ and Cs₈Na₁₆Ge₁₃₆ were somewhat ambiguous and inconclusive (27). The room temperature resistivities of the two samples were measured at ca. 48 and 52 mΩ-cm, respectively, while the corresponding numbers at 50 K were 30 and 45 mΩ-cm. Although indicating metallic behavior, the temperature dependence in both cases is very close to linear with slopes of 0.072 and 0.028 mΩ-cm/°C, respectively. Later, more accurate measurements were performed on single crystals and hot-pressed pellets of Cs₈Na₁₆Si₁₃₆. The numbers at room temperature were 30 and 90 μΩ-cm for a single crystal and a pellet, respectively, and clearly indicated a metallic state, which is in excellent agreement with the suggested electronic structure and stoichiometry. Four-probe measurements on two single crystals of Rb₈Na₁₆Si₁₃₆ at room temperature gave an average of 80 μΩ-cm, which is nearly identical to the resistivity of the Cs analog, as expected. It was not possible to measure over a wide temperature range since at lower temperatures the resistivity of the sample dropped out of the range of sensitivity of the measuring device. The resistivities of the two Ge clathrates were measured on a hot-pressed pellet for Rb₈Na₁₆Ge₁₃₆ and by the contact-free Q-method for Cs₈Na₁₆Ge₁₃₆. (The Q-method was also intended to serve as a reference for the four-probe measurements.) For the latter, the resistivity at room temperature was determined to be the order of 160 μΩ-cm, comparable with the resistivities measured for single crystals of the Si clathrates. The somewhat higher number is perhaps due to the numerous approximations such as assumptions for narrow particle size distribution and ideal spherical shape used for the calculations. The resistivity of the Rb₈Na₁₆Ge₁₃₆ pellet at room temperature was 110 μΩ-cm.

The results of the conductivity measurements are consistent with the temperature-independent Pauli

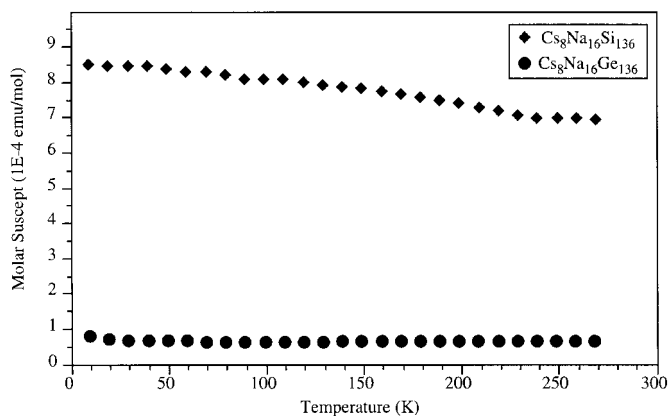


FIG. 3. Molar magnetic susceptibility (emu/mol) of $\text{Cs}_8\text{Na}_{16}\text{Si}_{136}$ and $\text{Cs}_8\text{Na}_{16}\text{Ge}_{136}$ as a function of the temperature (K) at a field of 3 T.

paramagnetism for all four phases. The plots of the molar magnetic susceptibilities versus the temperature are shown in Figs. 3 and 4. The raw data for all measurements were corrected for the holder and for the ion-core diamagnetism of Na^+ , Cs^+ , Rb^+ , Si^{4+} , and Ge^{4+} . No superconductivity at low fields (0.1–0.3 T) and low temperatures down to 2 K were found. These results are in agreement with previous measurements on $\text{Na}_8\text{Si}_{46}$ and $\text{Na}_x\text{Si}_{136}$ (22,24). The Pauli-like temperature-independent paramagnetism and metallic conductivity of $\text{Cs}_8\text{Na}_{16}\text{Si}_{136}$, $\text{Cs}_8\text{Na}_{16}\text{Ge}_{136}$, $\text{Rb}_8\text{Na}_{16}\text{Si}_{136}$, and $\text{Rb}_8\text{Na}_{16}\text{Ge}_{136}$ combined with the diamagnetic semiconducting behavior of the nonstoichiometric phase $\text{Na}_x\text{Si}_{136}$ prove that the alkali metal does not form an impurity band near the bottom of the framework conduction band. Rather, it supports the idea that there are strong charge-transfer interactions between the Si(Ge) and the alkali metal atoms, although the resulting structure can not be considered entirely ionic. Apparently, the involvement of the unoccupied p orbitals of the alkali metals in the empty

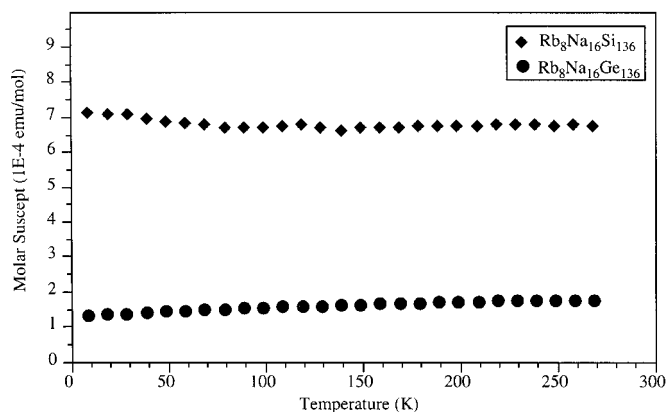


FIG. 4. Molar magnetic susceptibility (emu/mol) of $\text{Rb}_8\text{Na}_{16}\text{Si}_{136}$ and $\text{Rb}_8\text{Na}_{16}\text{Ge}_{136}$ as a function of the temperature (K) at a field of 3 T.

states of the network becomes more important, as shown from theoretical calculations (14,35,38).

As already discussed, the clathrates are considered promising thermoelectric materials because of the belief that “the rattling of the doping atoms within the voids of the structure” would improve their thermoelectric performance (31). In the context of this idea, the larger equivalent isotropic displacement parameter for the alkali metals residing in the clathrate-II cages indicates larger mean-square displacement amplitude of the corresponding atom, averaged over all directions. This is in agreement with the fact that the sodium thermal parameters in the Ge clathrates are larger than those in the Si clathrates. Sodium has an ionic radius of 1.02 Å, which fits the smaller cage for the silicon clathrates ($r_{\text{vanderWaals}} \approx 1.10$ Å) better than that of the germanium clathrates ($r_{\text{vanderWaals}} \approx 1.25$ Å). Also, the rubidium thermal parameters are larger than those of cesium in both the silicon and germanium structures. This, of course, should be expected since the lattice parameters for the Cs and Rb clathrates are nearly identical. Cs^+ with a radius of 1.70 Å fits better in the larger cage than Rb^+ with a radius 1.49 Å for both silicon and germanium clathrates with vander Waals radii the large cage of 1.85 and 2.00 Å, respectively (Table 6). This also accounts for the larger thermal parameter for Cs in **2** than in **1**. These oversized cages, with respect to the cations, are believed to be responsible for the good thermoelectric efficiency as demonstrated for some clathrate-I phases (e.g., $\text{Sr}_8\text{Ga}_{16}\text{Ge}_{30}$) (39) and some filled skutterudites (mineral structures with voids, e.g., $\text{LaFe}_4\text{Sb}_{12}$) (40). For maximum performance ($ZT > 1$), high thermopower and high electrical and low thermal conductivity would be required. However, good conductors of electricity are usually good conductors of heat as well, whereas the thermopower reaches its maximum for small band-gap semiconductors. Therefore, the results from the four-probe conductivity measurements discussed above imply that clathrate-II will not have high thermopower at room temperature, similar to that of $\text{Na}_x\text{Si}_{136}$ (about -100 $\mu\text{V}/\text{K}$) (22) or that of clathrate-I $\text{Sr}_8\text{Ga}_{16}\text{Ge}_{30}$ (-320 $\mu\text{V}/\text{K}$) (39), for instance. Figure 5 shows the thermopower of a cold-pressed pellet of $\text{Cs}_8\text{Na}_{16}\text{Si}_{136}$ versus the temperature. Indeed, the value at room temperature, -29 $\mu\text{V}/\text{K}$, is clearly not favorable for high thermoelectric efficiency. The slope, as expected, is negative, -0.07 $\mu\text{V}/\text{K}^2$, and indicates n -type conductivity. Simple calculations show that to have $ZT \geq 1$ at room temperature, our sample should have thermal conductivity of $\lambda \leq 0.8$ $\text{W}/\text{m}\cdot\text{K}$.

Why are there so many compounds with the clathrate-I structure and so few of clathrate-II structure? What is the reason for the preferred formation of one over the other? After all, as already pointed out, their stoichiometries are very similar, $\text{ATt}_{5.75}$ vs $\text{ATt}_{5.67}$. For the gas and liquid hydrates, it is well known that the size of the guest and the available volume of the host determine which clathrate will

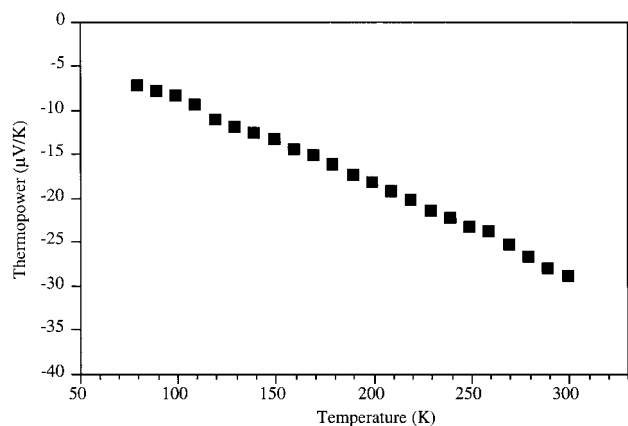


FIG. 5. Thermopower ($\mu\text{V/K}$) of $\text{Cs}_8\text{Na}_{16}\text{Si}_{136}$ as a function of the temperature (K).

form. The same, i.e., the relative sizes of the guest cation and the host cavity, play an essential role in the formation of intermetallic clathrates as well. Apparently, the electronic effects are not important since the A - Tt interactions are more or less purely electrostatic and similar for all alkali metals (except Li). Furthermore, since the Tt - Tt distances are similar for both clathrate types and are independent of the size of the cation, the volume of the $[5^{12}]$ polyhedra will be almost the same in both structures. Also, since there are two types of cages in each clathrate, two alkali metals will be preferred for their formation and stabilization. Therefore, the choice of cations with appropriate sizes and in appropriate ratios will be the product-directing factors. Thus, cations of only one size as in binary A - Tt systems stabilize the structure with cavities of similar sizes, i.e., that of clathrate-I, even when the reactions are designed to produce clathrate-II. Also, different cations but with similar sizes will stabilize clathrate-I as well. The smaller sodium and potassium form clathrate-I with the smaller silicon and germanium, while the larger rubidium and cesium match with tin. Since the two types of cavities in clathrate-II are quite different in size, on the other hand, its formation will be facilitated by a combination of cations with very different sizes. The radius of the smaller cavity in Si and Ge phases is comparable only with the radii of Na^+ and Na^+ or K^+ , respectively. Both Rb^+ and Cs^+ are too large to be incorporated into these cages but they can fit well into the larger $[5^{12}6^4]$ -hexakaidecahedra. No single size cation can fit efficiently enough in both cavities of clathrate-II. Bearing this idea in mind and moving one period down in group 14, one comes across Sn, where both cavities are large enough to be filled with Rb^+ and Cs^+ but too large for Na^+ and therefore no Na-Rb-Sn and Na-Cs-Sn clathrates of both types shall be expected. We can speculate that tin will most likely form only clathrate-I, mainly with Rb and/or Cs. This structure would be more stable than clathrate-II since the size of the larger void in the latter is too big ($r_{\text{vanderWaals}} > 2.2 \text{ \AA}$), even for a large

cation like Cs^+ . Therefore, the most reoccurring compounds in the binary and pseudo-binary systems A -Sn are clathrate-I and the clathrate-like phase $A_{8 \pm x}\text{Sn}_{25}$, containing chains of Sn dodecahedra only.

Prior to this work, the synthesis of phases with the clathrate-II structure such as $\text{Na}_x\text{Si}_{136}$ was done by the thermal decomposition of the Zintl compounds NaSi at high temperatures (300–400°C) and dynamic vacuum. The resulting products are usually inhomogeneous powders with undefined stoichiometry and contain both clathrate structures and unreacted NaSi, and even the elements, and further purification is necessary to separate the phases. Furthermore, small changes in the experimental conditions result in quite different overall compositions of the mixtures, and therefore poor reproducibility. Powder diffraction in this case is not a very useful tool for stoichiometry confirmation since the composition could vary substantially from particle to particle without noticeable changes in the lattice parameters due to the rigidity and covalency of the framework. Following the approach described above about the guest-host interactions, one can design compositions that are promising for the synthesis of clathrate-II: $\text{Cs}_8\text{Na}_{16}\text{Si}_{136}$, $\text{Cs}_8\text{Na}_{16}\text{Ge}_{136}$, $\text{Rb}_8\text{Na}_{16}\text{Si}_{136}$, $\text{Rb}_8\text{Na}_{16}\text{Ge}_{136}$, $\text{Cs}_8\text{K}_{16}\text{Ge}_{136}$, and $\text{Rb}_8\text{K}_{16}\text{Ge}_{136}$. Nevertheless, only the first four compounds were successfully synthesized. All reactions, intended to produce $\text{Cs}_8\text{K}_{16}\text{Ge}_{136}$ and $\text{Rb}_8\text{K}_{16}\text{Ge}_{136}$, failed, and the products were unreacted Ge and the known Zintl compounds $\text{K}_{12}\text{Ge}_{17}$ and $\text{Cs}_{12}\text{Ge}_{17}$ (or $\text{Rb}_{12}\text{Ge}_{17}$). Apparently, the existence of these stable phases obscures the eventual formation of clathrates of any type for both K-Rb-Ge and K-Cs-Ge.

Following the same size relations, we also designed some stoichiometric mixtures favorable for the formation of clathrate-I (Table 6). These proposed compositions are $\text{Na}_8\text{Si}_{46}$, K_8Si_{46} , $\text{Na}_2\text{K}_6\text{Si}_{46}$, $\text{Na}_2\text{Rb}_6\text{Si}_{46}$, $\text{Na}_2\text{K}_6\text{Ge}_{46}$, $\text{Na}_2\text{Rb}_6\text{Ge}_{46}$, $\text{Na}_2\text{Cs}_6\text{Ge}_{46}$, K_8Ge_{46} , $\text{K}_2\text{Rb}_6\text{Ge}_{46}$, $\text{K}_2\text{Cs}_6\text{Ge}_{46}$, $\text{K}_2\text{Rb}_6\text{Sn}_{46}$, $\text{K}_2\text{Cs}_6\text{Sn}_{46}$, $\text{Rb}_2\text{Cs}_6\text{Sn}_{46}$, K_8Sn_{46} , $\text{Rb}_8\text{Sn}_{46}$, and $\text{Cs}_8\text{Sn}_{46}$. All of them, excluding those that were already reported (Table 1), were tried and the results confirmed the importance of the choice of cations. The loading stoichiometry proved to be less important than the type of the available cations. Thus, reactions loaded with stoichiometries $\text{Na}_2\text{Rb}_6\text{Si}_{46}$, $\text{Na}_2\text{Rb}_6\text{Ge}_{46}$, and $\text{Na}_2\text{Cs}_6\text{Ge}_{46}$ and intended to produce clathrate-I yielded instead clathrate-II. These results are somewhat understandable, keeping in mind that the calculated relative thermodynamic stability of the two clathrate structures are nearly equal, with slight preference toward type-II. Changing the temperature profile or slightly modifying the ratio for these three systems led to the formation of stable $A_{12}\text{Ge}_{17}$ phases, similar to the results in $\text{Na}_2\text{K}_6\text{Ge}_{46}$, $\text{K}_2\text{Rb}_6\text{Ge}_{46}$, and $\text{K}_2\text{Cs}_6\text{Ge}_{46}$. Only a Na-K-Si reaction afforded the formation of clathrate-I, but in low yield and as

a fine powder. In the case of the *A*-Sn systems, two major phases comprised the results from nearly all reactions. These are the clathrate-like $A_{8\pm x}Sn_{25}$ and clathrate-I A_8Sn_{44} compounds (21). For instance, the products of $K_2Rb_6Sn_{46}$ were the two clearly distinguished phases $K_{8\pm x}Sn_{25}$ and $K_xRb_{8-x}Sn_{44}$ (or Rb_8Sn_{44}), which were identified from both powder XRD and single crystals. There is considerable sensitivity to the cation size. Apparently, due to the quite similar sizes of the K and Rb cations, a wide degree of mixing occurs, which was confirmed from the slightly shifted lines in the XRD powder patterns and in agreement with the results for the K-Cs-Sn systems (21). The observation that the K cations are preferably located (about 2/3 of occupancy) within the small cavity in $K_{1.6(1)}Cs_{6.4(1)}Sn_{44}$ while the Cs cations occupy the tetrakaidcahedra may also serve as proof of the above-discussed cation-size relations.

The composition $Rb_2Cs_6Sn_{46}$ was also examined and yielded clathrate-I, as predicted, in nearly 100% yield. The crystals looked rather shiny and had a metallic luster rather than the "dark gray appearance" of the tin clathrates previously described. To our surprise they turned out to be also stable at ambient conditions, oxygen, moisture, etc., contrary to the initially suggested sensitivity. Selected crystals were soaked in water for more than 12 h and they retained their quality. Moreover, careful measurements of the positions of the lines in the powder pattern revealed a lattice parameter somewhat larger ($a = 12.200(1) \text{ \AA}$) than those of the previously reported Cs_8Sn_{46} , $K_{1.6(1)}Cs_{6.4(1)}Sn_{44.0(1)}$, and $Rb_8Sn_{44.6(1)}$ with $a = 12.096(1)$, $12.084(1)$, and $12.054(1) \text{ \AA}$, respectively. Single-crystal X-ray diffraction data were collected, and the structure was refined as a defect Cs-Sn clathrate-I structure with exactly two tin vacancies per formula, i.e., $Cs_8Sn_{44}\square_2$ ($\square = \text{vacancy}$). The refinements were entirely routine and revealed fractional occupancy for the Sn *6c* site only (41). The Sn-Sn distances in $Cs_8Sn_{44}\square_2$ are longer than those in $Rb_8Sn_{44}\square_2$. The refinement carried out with variable site occupancy of the *6c* site resulted in 61(1) % site occupation for $Cs_8Sn_{44}\square_2$ compared to 77(2) % for $Rb_8Sn_{44}\square_2$ (21). Therefore, the corresponding formulas are $Cs_8Sn_{43.6(1)}$ vs $Rb_8Sn_{44.6(1)}$. The resistivity of $Cs_8Sn_{43.6(1)}$ was measured on a cold-pressed pellet made from selected crystals. The room temperature value, $320 \mu\Omega\text{-cm}$, is consistent with the reported resistivity of $K_{1.6(1)}Cs_{6.4(1)}Sn_{44.0(1)}$, $288 \mu\Omega\text{-cm}$ (21). It differs significantly from the resistivity of $Cs_8Zn_4Sn_{42}$, $52 \text{ m}\Omega\text{-cm}$ (42), although both compounds are expected to exhibit similar properties typical for electronically balanced Zintl compounds. Apparently, substitution of the *Tt* atoms with electron-poorer elements balances the charges more efficiently than that in phases with vacancies. The estimated semiquantitative band gaps for $K_{1.6}Cs_{6.4}Sn_{44}$ and for Cs_8Sn_{44} , $E_g \approx 0.25$ and $E_g \approx 0.07$ eV, respectively, either indicate different carrier concentrations, implied from the

slight differences in refinement on the partially occupied Sn site, or might be attributed to experimental errors. Nevertheless, the measured temperature-independent diamagnetism of the Cs_8Sn_{44} at a field of 3-T down to a temperature of 10 K confirms the structure refinement and the suggested stoichiometry $Cs_8Sn_{44}\square_2$, which had been previously reported as Cs_8Sn_{46} (43).

The clathrate-I phases with vacancies are typical for the binary and pseudo-binary *A*-Sn systems, while as already discussed, clathrate-I compounds of Si and the alkali metals are believed to be "defect-free" (16). Germanium clathrates are somewhat on the border line and the structure-properties relations for the *A*-Ge systems are still questionable. To clarify the electronic structures and the properties of the binary *A*-Ge clathrates-I and to compare them with those of the *A*-Si and *A*-Sn clathrates, we tried to synthesize the binary K_8Ge_{46} from pure elements. Unfortunately, all attempts were unsuccessful. However, a reaction carried out in Ga flux readily produced $K_8Ga_8Ge_{38}$ with a clathrate-I structure in high yield and good crystal quality. Data were collected and the structure was refined routinely without fractionally occupied network sites. Since Ge and Ga cannot be distinguished, the stoichiometry $K_8Ga_8Ge_{38}$ was deduced from the fact that the unit cell parameter ($a = 10.7706(5) \text{ \AA}$) (44) was invariant with respect to the amount of Ga loaded. Furthermore, the unit cell is slightly larger than the unit cell of K_8Ge_{46} ($a = 10.71 \text{ \AA}$) (11) but compares well with the cell parameters of $K_8Al_8Ge_{38}$ (45) and $K_8In_8Ge_{38}$ (46), $a = 10.785(1)$ and $11.033(2) \text{ \AA}$, respectively. Also, four-probe resistivity measurements on a cold-pressed pellet gave $\rho_{293} \approx 0.37 \Omega\text{-cm}$ and its temperature dependence clearly indicated a semiconducting state.

CONCLUSIONS

For the first time, large single crystals of $Cs_8Na_{16}Si_{136}$, $Cs_8Na_{16}Ge_{136}$, $Rb_8Na_{16}Si_{136}$, and $Rb_8Na_{16}Ge_{136}$ clathrate-II compounds have been synthesized from pure elements. The rational synthesis is reproducible and quantitative. The structures of these four compounds were elucidated with high accuracy from single-crystal X-ray diffraction data and the refinements unambiguously confirmed the first "defect-free and fully stuffed" clathrate-II structures. The measured transport and magnetic properties are consistent with the suggested ideal clathrate-II stoichiometry and indicate that these compounds do not have a future as thermoelectric materials. Our report on the clathrate exploration also adds some more information on the structural chemistry of silicon and germanium and tin at negative oxidation states. Thus, until now, in the systems alkali metal(s)-silicon, alkali metal(s)-germanium, and alkali metal(s)-tin, proven to exist by single-crystal X-ray diffraction, are Tt_4^{4-} tetrahedra, Tt_9^{4-} deltahedra (mono-capped square antiprisms or tricapped trigonal prisms) (47),

Tt_{25}^{8-} clathrate alike chiral chains, and clathrate-I (21) and clathrate-II frameworks, formally Tt_{46}^{8-} and Tt_{34}^{3-} in type I and type II, respectively.

ACKNOWLEDGMENTS

We thank John Greedan and his co-workers (McMaster University, Hamilton, Ontario) for the thermopower measurements, Paul Maggard (Iowa State University, Ames) for the Q-measurements, the donors of The Petroleum Research Fund administered by the ACS for support of this research, and the NSF for an equipment grant (DMR-9703732) for the SQUID magnetometer.

REFERENCES

- M. L. Cohen and T. L. Bergstresser, *Phys. Rev.* **141**, 789 (1966); J. I. Pankove, "Optical Processes in Semiconductors." Dover, New York, 1975. T. G. Brown and D. G. Hall, *Appl. Phys. Lett.* **49**, 245 (1986).
- A. P. Alivisatos, *Science* **271**, 933 (1996); J. R. Health, J. J. Shiang, and A. P. Alivisatos, *J. Chem. Phys.* **101**, 1067 (1994); L. E. Brus, P. F. Szajowski, W. L. Wilson, T. D. Harris, S. Schuppler, and P. H. Citrin, *J. Am. Chem. Soc.* **117**, 2915 (1995).
- L. T. Canham, *Appl. Phys. Lett.* **57**, 1046 (1990); A. G. Cullis, L. T. Canham, and P. D. Calcot, *J. Appl. Phys.* **82**, 909 (1997).
- M. S. Hybertsen, *Phys. Rev. Lett.* **72**, 1514 (1994); T. Takagahara and K. Takeda, *Phys. Rev. B* **46**, 15578 (1992). B. Delyly and E. F. Steigemeier, *Phys. Rev. B* **47**, 1397 (1993).
- Y. Guyot, B. Champagnon, E. Reny, C. Cros, M. Pouchard, P. Melinon, A. Perez, and I. Gregora, *Phys. Rev. B* **57**, 9475 (1998); R. G. Mathur, R. M. Mehra, and P. C. Mathur, *J. Appl. Phys.* **83**, 5855 (1998).
- J. C. Jamieson, *Science* **139**, 762 (1963).
- H. Davy, *Philos. Trans. R. Soc. London* **101**, 155 (1811).
- M. Faraday, *Q. J. Sci.* **15**, 71 (1823).
- W. F. Claussen, *J. Chem. Phys.* **19**, 1425 (1951); L. Pauling and R. E. Marsh, *Proc. Natl. Acad. Sci. U.S.A.* **36**, 112 (1952); M. von Stackelberg, O. Gotzen, J. Pietuchovsky, O. Witscher, H. Fruhbuss, and W. Meinhold, *Fortschr. Mineral.* **26**, 122 (1947).
- J. S. Kasper, P. Hagenmuller, M. Pouchard, and C. Cros, *Science* **150**, 1713 (1965); C. Cros, M. Pouchard, and P. Hagenmuller, *Compt. Rend.* **260**, 4764 (1965).
- J. Gallmeier, H. Schäfer, and A. Weiss, *Z. Naturforsch.* **24b**, 665 (1969).
- P. Villars and L. D. Calvers, Eds. "Pearson's Handbook of Crystallographic Data for Intermetallic Phases." ASM International: Materials Park, OH, 1991.
- R. Nesper, K. Vogel, and P. E. Blöchl, *Angew. Chem. Int. Ed. Engl.* **32**, 701 (1993); M. O'Keeffe, G. B. Adams, and O. F. Sankey, *Phys. Rev. Lett.* **68**, 2325 (1992).
- A. A. Demkov, W. Windl, and O. F. Sankey, *Phys. Rev. B* **53**, 11288 (1996); A. A. Demkov, O. F. Sankey, K. E. Schmidt, G. B. Adams, and M. O'Keeffe, *Phys. Rev. B* **50**, 17001 (1994); M. O'Keeffe, G. B. Adams, and O. F. Sankey, *Philos. Mag. Lett.* **78**, 21 (1998).
- R. M. Fleming, M. J. Rosseinsky, A. P. Ramirez, D. W. Murphy, R. C. Haddon, S. M. Zahurak, and A. V. Makhija, *Nature* **352**, 787 (1991). P. W. Stephens, L. Mihaly, P. L. Lee, R. L. Whetten, S. M. Huang, R. Kaner, F. Diedrich, and K. Holczer, *Nature* **351**, 632 (1991); M. J. Rosseinsky, D. W. Murphy, R. M. Fleming, R. Tycko, A. P. Ramirez, T. Siegrist, G. Dabbagh, and S. E. Barrett, *Nature* **356**, 416 (1992).
- G. K. Ramachandran, J. Dong, J. Diefenbacher, J. Gryko, R. F. Marzke, O. F. Sankey, and P. F. McMillan, *J. Solid State Chem.* **145**, 716 (1999); G. K. Ramachandran, P. F. McMillan, J. Diefenbacher, J. Gryko, J. Dong, and O. F. Sankey, *Phys. Rev. B* **60**, 12294 (1999).
- N. F. Mott, *J. Solid State Chem.* **6**, 348 (1973).
- H.-G. von Schnering, *Nova Acta Leopold.* **59**, 168 (1985). H.-G. von Schnering, *Bol. Soc. Chil. Quim.* **33**, 41 (1988).
- R. Nesper and H.-G. von Schnering, *Tschermaks Mineral. Petrogr. Mitt.* **32**, 195 (1983).
- Some direct but unpublished verifications of A_8Tt_{44} compositions were brought to our knowledge with the courtesy of H.-G. von Schnering: J. Llanos, Doctoral Dissertation, University of Stuttgart, 1983. R. Kröner, Doctoral Dissertation, University of Stuttgart, 1989. M. Baitinger, Y. Grin, and H.-G. von Schnering, "Abstracts from the VI-th European Conference of Solid State Chemistry", Zürich, 1997, p. 116. ETH Zürich, Switzerland, 1997.
- J. T. Zhao and J. D. Corbett, *Inorg. Chem.* **33**, 5721 (1994).
- C. Cros, M. Pouchard, and P. Hagenmuller, *J. Solid State Chem.* **2**, 570 (1970).
- E. Reny, P. Gravereau, C. Cros, and M. Pouchard, *J. Mater. Chem.* **8**, 2839 (1998); E. Reny, M. Ménétrier, C. Cros, M. Pouchard, and J. Sénégas, *C. R. Acad. Sci. Sér. IIC*, 129 (1998).
- S. B. Roy, K. E. Sim, and A. D. Caplin, *Philos. Mag. B* **65**, 1445 (1992).
- J. Gryko, P. F. McMillan, R. F. Marzke, A. P. Dodokin, A. A. Demkov, and O. F. Sankey, *Phys. Rev. B* **57**, 4172 (1998).
- R. Kröner, K. Peters, H.-G. von Schnering, and R. Nesper, *Z. Kristallogr. NCS* **213**, 664 (1998).
- S. Bobev and S. C. Sevo, *J. Am. Chem. Soc.* **121**, 3795 (1999).
- H. Kawaji, H. Horie, S. Yamanaka, and M. Ishikawa, *Phys. Rev. Lett.* **74**, 1427 (1995); H. Kawaji, K. Iwai, S. Yamanaka, and M. Ishikawa, *Solid State Commun.* **100**, 393 (1996); H. Yahiro, K. Yamaji, M. Shiotani, S. Yamanaka, and M. Ishikawa, *Chem. Phys. Lett.* **246**, 167 (1995); F. Shimizu, Y. Maniwa, K. Kume, H. Kawaji, S. Yamanaka, and M. Ishikawa, *Phys. Rev. B* **54**, 13242 (1996); S. L. Fang, L. Grigorian, P. C. Eklund, G. Dresselhaus, M. S. Dresselhaus, H. Kawaji, and S. Yamanaka, *Phys. Rev. B* **57**, 7686 (1998). D. Kahn and J. P. Lu, *Phys. Rev. B* **56**, 13898 (1997).
- S. Yamanaka, E. Enishi, H. Fukuoka, and M. Yasukawa, *Inorg. Chem.* **39**, 56 (2000).
- A. San-Miguel, P. Keghelian, X. Blase, P. Melinon, A. Perez, J. P. Itie, A. Polian, E. Reny, C. Cros, and M. Pouchard, *Phys. Rev. Lett.* **83**, 5290 (1999).
- G. A. Slack, *Solid State Phys.* **34**, 1 (1979); D. M. Rowe, Ed. "CRC Handbook of Thermoelectrics." CRC Press, Boca Raton, FL, 1995; G. A. Slack, in "Thermoelectric Materials—New Directions and Approaches" (T. M. Tritt, M. G. Kanatzidis, H. B. Lyon, and G. D. Mahan, Eds.), MRS Symposium Proceedings, Vol. 478, p. 47. MRS: Pittsburgh, PA, 1997.
- Caution: Such reactions lead to high pressure in the niobium container and may result in a leak of alkali metal into the silica ampoules. The latter should be made sufficiently long, and one of its ends should be left protruding outside the furnace for condensation of alkali metals in case a leak occurs.
- SHELXTL, Version 5.1, Bruker Analytical X-Ray Systems, Inc., 1997.
- G. B. Adams, M. O'Keeffe, A. A. Demkov, O. F. Sankey, and Y.-M. Huang, *Phys. Rev. B* **49**, 8048 (1994).
- J. D. Dong and O. F. Sankey, *J. Phys.: Condens. Matter* **11**, 6129 (1999).
- L. Pauling, "The Nature of the Chemical Bond," 3rd ed. Cornell Univ. Press, Ithaca, NY, 1960.
- J. Gryko, P. F. McMillan, and O. F. Sankey, *Phys. Rev. B* **54**, 3037 (1996).
- V. I. Smelyanski and J. S. Tse, *Chem. Phys. Lett.* **264**, 459 (1997).
- G. S. Nolas, J. L. Cohn, G. A. Slack, and S. B. Schbujman, *Appl. Phys. Lett.* **73**, 178 (1998).
- W. Jetschko and D. Braun, *Acta Crystallogr. B* **33**, 3401 (1977). B. C. Sales, D. Mandrus, and R. K. Williams, *Science* **272**, 1325 (1996).

41. An octant of X-ray diffraction data from a single crystal of $\text{Cs}_8\text{Sn}_{46}$ ($0.10 \times 0.10 \times 0.08$ mm, $2\theta_{\text{max}} = 50^\circ$) were collected on a CAD-4 at room temperature with monochromated $\text{MoK}\alpha$ radiation. The structure was refined as $\text{Cs}_8\text{Sn}_{43.6(1)}$. No evidence for Rb content was found; the compound can be made in a rational way from Cs and Sn only. Crystal data: $Pm\bar{3}n$, No. 223, $Z = 1$, $a = 12.200(1)$ Å, $\mu = 187.61$ cm $^{-1}$, $d_{\text{calc}} = 5.748$ g cm $^{-3}$, $R_1/wR_2 = 3.21/6.94\%$ and $4.22/7.22\%$ for 300 observed ($I \geq 2\sigma_I$) and 347 total number of reflections, respectively, and 16 variables, including the extinction coefficient. Important Sn-Sn distances: Sn1-Sn1 = 2.876(2); Sn1-2Sn1 = 2.8494(7); Sn1-Sn3 = 2.7981(9); Sn2-3Sn1 = 2.8494(7); Sn2-Sn2 = 2.826(2); Sn3-4Sn1 = 2.7981(9) Å.
42. G. S. Nolas, T. J. R. Weakley, and J. L. Cohn, *Chem. Mater* **11**, 2470 (1999).
43. Y. Grin, L. Z. Melekhov, K. A. Chuntanov, and S. P. Yatsenko, *Sov. Phys. Crystallogr.* **32**, 290 (1987).
44. An octant of X-ray diffraction data from a single crystal of $\text{K}_8\text{Ga}_8\text{Ge}_{38}$ ($0.16 \times 0.14 \times 0.14$ mm $2\theta_{\text{max}} = 50^\circ$) were collected on a CAD-4 at room temperature with monochromated $\text{MoK}\alpha$ radiation. The structure was refined as fully occupied $\text{K}_8\text{Ga}_8\text{Ge}_{38}$. Crystal data: $Pm\bar{3}n$, No. 223, $Z = 1$, $a = 10.7706(5)$ Å, $\mu = 273.43$ cm $^{-1}$, $d_{\text{calc}} = 4.823$ g cm $^{-3}$, $R_1/wR_2 = 2.09/4.02\%$ and $4.49/4.14\%$ for 156 observed ($I \geq 2\sigma_I$) and 220 total number of reflections, respectively, and 16 variables, including the extinction coefficient. Important Ge-Ge distances: Ge1-Ge1 = 2.537(1); Ge1-2Ge1 = 2.4936(4); Ge1-Ge3 = 2.5105(5); Ge2-3Ge1 = 2.4936(4); Ge2-Ge2 = 2.467(1); Ge3-4Ge1 = 2.5105(5) Å.
45. R. Kröner, K. Peters, H.-G. von Schnering, and R. Nesper, *Z. Kristallogr. NCS* **213**, 675 (1998).
46. H.-G. von Schnering, H. Menke, R. Kröner, E. M. Peters, K. Peters, and R. Nesper, *Z. Kristallogr. NCS* **213**, 673 (1998).
47. H. Schäfer, *Annw. Rev. Mater. Sci.* **15**, 1 (1985), and references therein; V. Quéneau and S. C. Sevov, *Angew. Chem. Int. Ed. Engl.* **36**, 1754 (1997); V. Quéneau, E. Todorov, and S. C. Sevov, *J. Am. Chem. Soc.* **120**, 3263 (1998).
48. W. Westerhaus and H.-U. Schuster, *Z. Naturforsch.* **32b**, 1365 (1977).
49. H.-G. von Schnering, R. Kröner, H. Menke, K. Peters, and R. Nesper, *Z. Kristallogr. NCS* **213**, 677 (1998).
50. H.-G. von Schnering, W. Carrillo-Cabrera, R. Kröner, K. Peters, E.-M. Peters, and R. Nesper, *Z. Kristallogr. NCS* **213**, 679 (1998).
51. R. Kröner, K. Peters, H.-G. von Schnering, and R. Nesper, *Z. Kristallogr. NCS* **213**, 667 (1998).
52. B. Eisenmann, H. Schäfer, and R. Zagler, *J. Less-Common. Met.* **118**, 43 (1986).
53. B. Kuhl, A. Czybulka, and H.-U. Schuster, *Z. Anorg. Allg. Chem.* **621**, 1 (1995).
54. H. Menke and H.-G. von Schnering, *Z. Anorg. Allg. Chem.* **395**, 223 (1973).
55. M. M. Shartuk, K. A. Kovnir, A. V. Shevelkov, I. A. Presniakov, and B. A. Popovkin, *Inorg. Chem.* **38**, 3455 (1999).
56. R. Nesper, J. Curda, and H.-G. von Schnering, *Angew. Chem.* **98**, 369 (1986); *Angew. Chem. Int. Ed. Engl.* **25**, 350 (1986).
57. R. F. W. Herrmann, K. Tanigaki, S. Kuroshima, and H. Suematsu, *Chem. Phys. Lett.* **283**, 29 (1998).
58. R. Kröner, K. Peters, H.-G. von Schnering, and R. Nesper, *Z. Kristallogr. NCS* **213**, 669 (1998).
59. R. Kröner, K. Peters, H.-G. von Schnering, and R. Nesper, *Z. Kristallogr. NCS* **213**, 671 (1998).
60. J. Dünner and A. Mewis, *Z. Anorg. Allg. Chem.* **621**, 191 (1995).
61. H. Menke, W. Carrillo-Cabrera, R. Kröner, K. Peters, E.-M. Peters, and H.-G. von Schnering, *Z. Kristallogr. NCS* **214**, 14 (1999).
62. R. D. Shannon and C. T. Prewitt, *Acta Crystallogr. B* **25**, 925 (1969).